Nuclear magnetic resonance quadrupolar parameters and short range order in disordered ionic fluorides

2000 J. Phys.: Condens. Matter 12 5775

(http://iopscience.iop.org/0953-8984/12/26/323)

J. Phys.: Condens. Matter **12** (2000) 5775–5788. Printed in the UK PII: S0953-8984(00)12368-9

Nuclear magnetic resonance quadrupolar parameters and short range order in disordered ionic fluorides

B Bureau†, G Silly†, J Y Buzaré†§, B Boulard‡ and C Legein‡

† Laboratoire de Physique de l'Etat Condensé, UPRES-A CNRS No 6087, Université du Maine, 72085 Le Mans Cédex 9, France

‡ Laboratoire des Fluorures, UPRES-A CNRS No 6010, Université du Maine, 72085 Le Mans Cédex 9, France

Received 6 March 2000

Abstract. Information on both radial and angular atomic coordinations is provided by the quadrupole interaction between the quadrupole moment of the atomic nuclei and the electric field gradients (EFGs) originating from the distribution of electric charges around the nuclei. ^{69}Ga and ^{71}Ga are quadrupolar nuclei active in NMR. Their spectra are recorded in amorphous GaF_3 which may be considered as a model compound for disordered fluorides with fluorine corner sharing octahedra. An unique and continuous quadrupolar parameter Czjzek distribution allows us to simulate the experimental spectra. The measured chemical shifts indicate that the Ga^{3+} ions are at the centre of $(GaF_6)^{3-}$ octahedra in the amorphous GaF_3 phase.

A polarizable point charge model is used to explain NMR quadrupolar parameters which are related to the electric field gradients at the Ga site. Lattice summations are performed in the direct space over spherical volumes. Atomic position sets generated by molecular dynamics are shown to give quadrupolar parameter distributions which look like Czjzek ones whatever the EFG calculation approximations. Provided the polarizabilities are adjusted, they allow us to reconstruct the experimental NMR spectra which correspond in any case to slightly distorted $(GaF_6)^{3-}$ octahedra. The present approach may be applied to any ionic disordered compound which contains quadrupolar nuclei and used to quantify short range order around such nuclei.

1. Introduction

Most experimental data on the degree of short range ordering in disordered solids are usually obtained using diffraction techniques and EXAFS. The experimental results are determined by the number and radial distances of atoms in the first coordination shells but carry no information on their angular distribution. One possibility of yielding information on the angular atomic coordinations is provided by the quadrupole interaction between the quadrupole moment of the atomic nuclei and the electric field gradients (EFGs) originating from the distribution of electric charges around the nuclei.

Nuclei with spin greater than $\frac{1}{2}$ constitute a large group of NMR active nuclei in the periodic table. They are subjected to this quadrupole interaction and so they can be used as effective microscopic probes. Their potential as probe of structure in solids has been greatly enhanced with the recent development of high resolution techniques. However, relatively little is known about the relationships between the measured quadrupolar parameters ν_Q and η_Q, and the charge distributions. Publications trying to relate NMR quadrupolar parameters to structural

§ Corresponding author.

0953-8984/00/265775+14$30.00

features are rare [1, 2] despite this approach could be particularly useful in quantifying radial and angular atomic distributions in disordered phases such as amorphous and glassy materials.

It is important to emphasize that such an approach provides relevant local information but does not allow to strictly establish the structural long range order of disordered systems. To our knowledge, two alternatives may be worked out. A first one is based on first modelling some structural networks and then comparing so inferred quadrupolar parameters to experimental ones. Such an approach was used in the case of FeF_3 and quadrupolar parameters observed by Mössbauer spectrometry [3, 4]. A second one consists in modelling distributions of short range local structure which may account for the experimental quadrupolar parameter distribution: in this case molecular dynamics appears to be an extremely suitable route as will be discussed in the following sections. This latter approach has been previously used in the case of fluoride glasses and EPR fine structure parameters [5, 6].

In this paper, we concentrate on the amorphous phase of GaF_3. Since this compound is highly ionic, the EFG tensor components may be evaluated through charge summations using a polarizable point charge model. As it will be shown further, amorphous GaF_3 may be considered as a model compound for disordered ionic fluoride network built up from corner sharing fluorine octahedra such as transition metal fluoride glasses (TMFGs). Furthermore, due to their large quadrupolar interaction sensitivity to EFG, the ^{69}Ga and ^{71}Ga nuclei are good candidates to check the validity of the approach which is detailed in the following.

The paper is organized as follows. Experimental details are given in section 2. Section 3 introduces the way to reconstruct the NMR spectra with quadrupolar parameter distributions of Czjzek type. In section 4, disordered structures of GaF_3 are simulated through molecular dynamics (MD) and EFG calculations are developed using a polarizable point charge model for these structures. The influence of monopolar and dipolar approximations on the results is checked. Our calculations give evidence for the dependence of the results on the fluorine and gallium ionic polarizabilities, the Ga^{3+} Sternheimer constant and its nuclear quadrupole moment. Comparisons with the local order structure previously deduced from Mössbauer [3, 4] and EPR [5, 6] experiments are discussed and allow us to overcome these difficulties. It will be shown that our results are unable to mirror some frustrated topology as seen in magnetic amorphous FeF_3 by Mössbauer spectrometry [3, 4], but allow us to obtain quantitative information concerning angular and radial distortions of the GaF_6 octahedra.

2. Experiment

2.1. Materials

Amorphous GaF_3 was obtained by vapour phase deposition which was conducted in a 6 cm diameter Pyrex vessel connected to a vacuum system allowing pressure around 10^{-4} mbar in the vessel. The platinum crucible containing the starting rhombohedral crystalline phase of GaF_3 was heated with an RF coil.

2.2. NMR measurements

All the experiments were carried out at room temperature on a Bruker MSL 300 spectrometer (7.0 T). A commercial double bearing 4 mm MAS probe was used for both static and MAS (15 kHz) spectra.

Both ^{69}Ga and ^{71}Ga isotopes have $I = \frac{3}{2}$, their Larmor frequencies are 72.003 and 91.491 MHz and their quadrupole moments $Q(^{69}\text{Ga}) = 0.17 \pm 0.01\ 10^{-28}$ m^2 and $Q(^{71}\text{Ga}) = 0.11 \pm 0.01\ 10^{-28}$ m^2, respectively. The error bars correspond to the dispersion of the

values found in the literature [7]. The definitions of the measured quadrupolar parameters are the following: the quadrupolar frequency is written $\nu_Q = 3eQV_{ZZ}/2I(2I-1)h$ and the asymmetry parameter is given by $\eta_Q = (V_{XX} - V_{YY})/V_{ZZ}$, where Q is the quadrupolar moment, V_{XX}, V_{YY} and V_{ZZ} are the principal components of the electric field gradient tensor, with the condition $|V_{ZZ}| \geqslant |V_{YY}| \geqslant |V_{XX}|$ leading to $0 \leqslant \eta_Q \leqslant 1$. The isotropic chemical shift δ_{iso} used for the spectrum simulation is defined as $\delta_{iso} = \frac{1}{3}(\delta_{xx} + \delta_{yy} + \delta_{zz})$: $\delta_{ii} = \sigma_{ref} - \sigma_{ii}$ where σ_{ii} $(i = x, y, z)$ are the principal components of the shielding tensor. For sixfold coordinated Ga, it was previously shown that δ_{aniso} is negligible versus η_Q [8–10].

K_2NaGaF_6, in which the Ga atoms stand at the centre of regular octahedra [11], is used as an external reference.

Due to the large quadrupolar interaction, the ^{69}Ga and ^{71}Ga static spectra in amorphous GaF_3 extend over more than 1 MHz. Thus, even the central $\langle -1/2, +1/2 \rangle$ lines are impossible to irradiate uniformly. Therefore, we used the so called VOCS (variable offset cumulative spectrum) method [12, 13]: the total spectrum is the sum of 15 full-echo spectra (t_{pulse}–τ–$2t_{pulse}$–acquisition) at offsets incremented by 150 kHz corresponding to a flat cumulative irradiation domain of 2 MHz. Each full echo is easily acquired due to its short duration in the time domain (less than 100 μs). Moreover, the magnitude computation of the full-echo Fourier transform leads directly to the correct absorption spectrum because the dispersive part is null. Although the full-echo acquisitions improve the signal-to-noise ratio, about 20 000 scans were necessary for each echo spectrum with a recycle delay of 250 ms. The radio-frequency field strength (100 kHz) was measured on a liquid containing Ga^{3+} ions (2.5 μs for $t_{\pi/2}$ liquid). The pulse length, t_{pulse}, was chosen much smaller than $t_{\pi/2}$ ($t_{\pi/2} \approx 3.5t_{pulse}$) to ensure a linear irradiation regime in order to avoid the distortion of the central transition [14, 15].

3. Experimental results

In terms of the second order quadrupolar effect which depends on ν_Q^2/ν_0, where ν_0 is the Larmor frequency, the ^{71}Ga spectrum at 7 T is equivalent to the ^{69}Ga one at 17.5 T. So, the ^{69}Ga VOCS spectrum is simply deduced from the ^{71}Ga corresponding one by a multiplication of the frequency scale by a factor of 3.2. Therefore, only ^{71}Ga spectra will be shown (figure 1(a)) and discussed in the following. The strongly asymmetrical broad line without any resolved structure corresponding to the ^{71}Ga VOCS in amorphous GaF_3 is quite similar to the one observed in PZG (PbF_2–ZnF_2–GaF_3) glasses [12]. So, Czjzek quadrupolar parameter distributions $P(\nu_Q, \eta_Q)$ [16, 17] previously involved in the simulation of ^{71}Ga NMR spectra in PZG glasses were also used here for amorphous GaF_3. The $P(\nu_Q, \eta_Q)$ expression is written

$$P(\nu_Q, \eta_Q) = \frac{1}{\sqrt{2\pi}\sigma^d} \nu_Q^{d-1} \eta_Q (1 - \eta_Q^2/9) \exp\left\{ -\frac{\nu_Q^2(1 + \eta_Q^2/3)}{2\sigma^2} \right\}$$

where σ and d are two adjustable parameters: σ characterizes the strength of the quadrupolar interaction and d, which is taken in the following as an integer number, corresponds to the number of independent components of the quadrupolar tensor ($d \leqslant 5$). A decrease of d from its maximum value of 5, mirrors local geometrical constraints which correlate the quadrupolar tensor components [17]. It appears that the distribution function $P(\nu_Q, \eta_Q)$ is null when ν_Q and/or η_Q are equal to zero. So, high symmetry electric field gradients are prohibited in agreement with the notion of disorder in this amorphous compound.

Simulations of both ^{69}Ga and ^{71}Ga NMR spectra in the amorphous phase of GaF_3 were performed using a modified version of the WINFIT Bruker software package developed by Massiot [18] who introduced the Czjzek distribution in the program [12]. The results were obtained with the following rules:

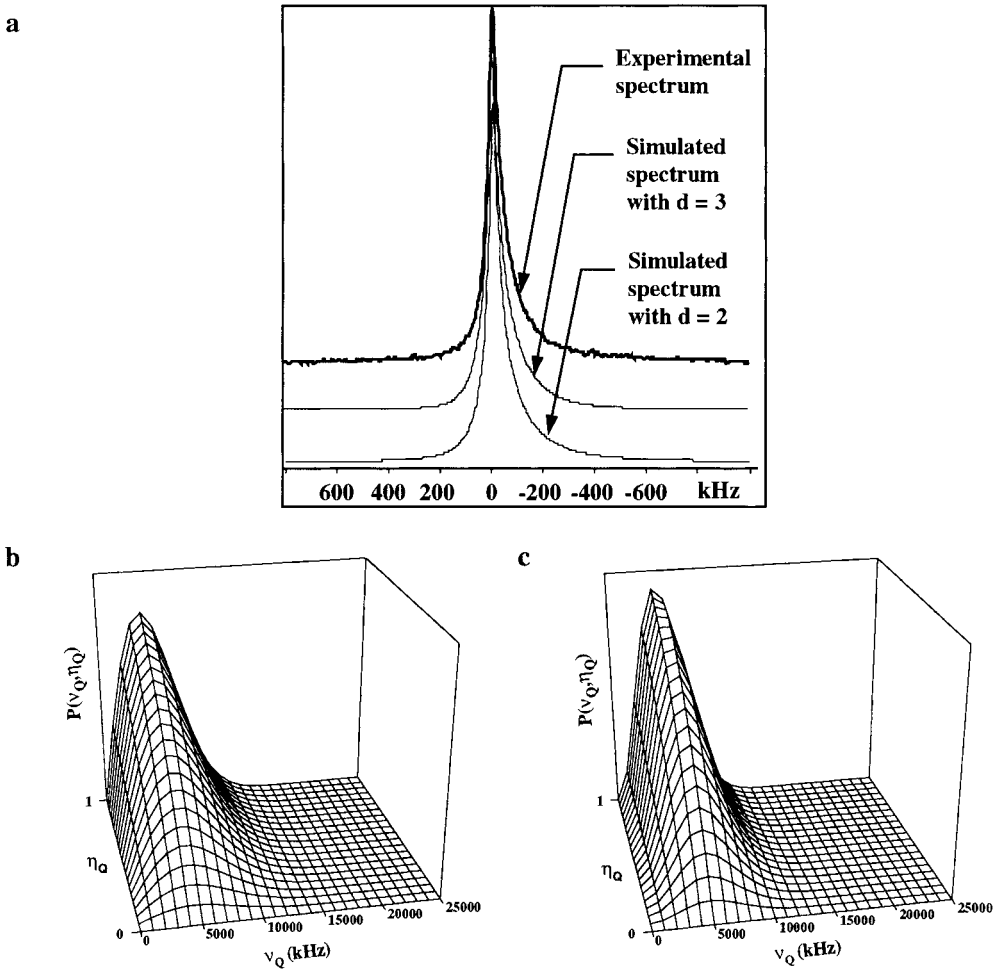

Figure 1. Experimental and simulated ^{71}Ga NMR spectra (a); Czjzek distributions used to calculate the simulated spectra: $d = 2$, $\sigma = 4500$ kHz (b); $d = 3$, $\sigma = 3500$ kHz (c).

- both the isotropic chemical shifts δ_{iso} and the asymmetry quadrupolar parameters η_Q have the same value for the two isotopes;
- when going from ^{71}Ga to ^{69}Ga, the σ value has to be multiplied by 1.55 which is equal to the ratio of the quadrupole constants of the two isotopes;
- in agreement with several previous results in fluoride glasses [12], we assumed that the Ga^{3+} ions are sixfold fluorine coordinated and an unique isotropic chemical shift value was considered.

Figure 1(a) shows the fine agreement between the calculated and experimental spectra obtained by using such distributions with 400 pairs of quadrupolar parameters (ν_Q, η_Q). The asymmetry of the spectrum is reproduced quite satisfactorily. This is not the case with Gaussian distributions of the quadrupolar parameters. The isotropic chemical shift value $\delta_{iso} = -65 \pm 5$ ppm confirms the sixfold fluorine co-ordination of Ga^{3+} ions in the amorphous GaF_3 phase. Two distributions with different d and σ values allowed us to reconstruct the spectrum: $d = 2$ and $\sigma = 4500$ kHz (figure 1(b)) or $d = 3$ and $\sigma = 3500$ kHz (figure 1(c)) for

^{71}Ga. For ^{69}Ga, we obtained $\sigma = 7300$ kHz for $d = 2$ or $\sigma = 5500$ kHz for $d = 3$. The error bar on σ is about 100 kHz. These parameters are close to those allowing the experimental Ga NMR spectra in PZG glasses to be reproduced: $d = 2$ and $\sigma = 4600$ kHz or $d = 3$ and $\sigma = 3650$ kHz for ^{71}Ga [12].

From these results, it may be inferred that the quadrupolar parameter distribution is a characteristic feature of the $(GaF_6)^{3-}$ octahedron distortion common to the two structures. The Zn^{2+} and Pb^{2+} ions, which are specific to the PZG glass structure do not influence the distribution. This means that the electric field gradient calculations described below for amorphous GaF_3 will be also valid for these glasses.

4. Electric field gradient and quadrupolar parameter calculation in amorphous GaF_3

In order to quantify the radial and angular octahedron distortions in such disordered ionic compounds and eventually to characterize the topological order, it is necessary to relate the quadrupolar parameters and the EFG at the Ga sites.

Some attempts have already been done to account for Mössbauer [3, 4, 19, 20] or EPR [5, 6] parameters which are related to EFG.

EFG calculations using a point charge model in the direct lattice have been developed in $AFe^{III}F_4$ (A = K, Cs, Rb, NH_4) [19] and MF_3 crystalline structures [20] at the dipolar approximation and in random corner sharing octahedra networks mirroring amorphous FeF_3 [3, 4] at the monopolar approximation only. The computed quadrupole parameter distribution compared well with experimental data from Mössbauer experiments under zero and high magnetic field. However, the experimental investigations are restricted to iron compounds.

In a work concerning quantification of the local order in PZG (PbF_2–ZnF_2–GaF_3) glasses [5, 6], the Cr^{3+} and Fe^{3+} EPR spectra were found to be very similar to those recorded in amorphous GaF_3, leading to the same conclusion drawn above from the NMR experiments that the local order around Ga in GaF_3 and PZG glasses are similar. This result prompted us to apply MD calculations on GaF_3 to simulate this local order. The empirical superposition model [21] was applied to calculate the fine structure parameter distributions from the radial and angular atomic coordinations of the nearest neighbours around the paramagnetic probes. It was then possible to obtain distributions of the EPR fine structure parameters and to reconstruct successfully the Cr^{3+} and Fe^{3+} EPR spectra in amorphous GaF_3 and in PZG glasses in agreement with the experimental spectra. It was shown that the constituent fluorine octahedra are only slightly distorted and that the distributions of the fine structure parameters are similar to the Czjzek ones used to simulate the Cr^{3+} and Fe^{3+} EPR spectra [6]. It may be noticed that in this study, no direct EFG calculations were made. Furthermore, one may suspect the paramagnetic probes to impose their own environment.

In the present work, the Ga site itself either in GaF_3 or in PZG glasses is investigated in order to quantify the disorder around Ga^{3+}. MD is applied to generate GaF_3 disordered phases. EFG calculations from these phases are used to correlate the measured quadrupolar parameters to the Ga site distortions. As in [3], [4], [15] and [16], EFG calculations are undertaken using a polarizable point charge model well adapted for ionic fluorides. This approach is expected to be valid for any quadrupolar nucleus involved in a disordered ionic structure.

4.1. Polarizable point charge model

In this model, ionic materials are assumed to consist of discrete deformable ions. The local electric field $\vec{E}$ acting on a given ion induces a dipole moment $\vec{P} = [\alpha_e]\vec{E}$ on it. Generally, the electronic polarizability tensor $[\alpha_e]$ is assumed to be isotropic. For an ion μ surrounded

by some λ ions with charges $q(\lambda)$ and electronic polarizabilities $\alpha_e(\lambda)$, one obtains

$$E_i(\mu) = \frac{1}{4\pi\varepsilon_0}\sum_{\lambda}\left[q(\lambda)X_i(\vec{R}_{\mu,\lambda}) + \sum_k \alpha_e(\lambda)E_k(\lambda)X_{ik}(\vec{R}_{\mu,\lambda}) + \cdots\right] \quad (1)$$

for the electric field components and

$$V_{ij}(\mu) = \frac{1}{4\pi\varepsilon_0}\sum_{\lambda}\left[q(\lambda)X_{ij}(\vec{R}_{\mu,\lambda}) + \sum_k \alpha_e(\lambda)E_k(\lambda)X_{ijk}(\vec{R}_{\mu,\lambda}) + \cdots\right] \quad (2)$$

for the EFG tensor components, with, $X_{\underbrace{k,1,\ldots}_{p\,indices}}(\vec{R}) = ((\partial^p/\partial x_k \partial x_1 \ldots)(1/r))_{r=R}$. This leads to a self-consistent problem. The first term in the brackets in equations (1) and (2) is the monopolar contribution; the second term is the dipolar one. We neglected higher order contributions. The summations over λ are performed on spherical volumes.

From equation (2), the six different components of the EFG tensor, V_{XX}, V_{YY}, V_{ZZ}, V_{XY}, V_{XZ} and V_{YZ} are calculated in the laboratory reference frame. Next, the EFG tensor is diagonalized by the Jacobi method, the three eigenvalues are arranged in the order $|V_{ZZ}| > |V_{YY}| > |V_{XX}$ and the relevant quadrupolar parameters $\nu_Q = (1-\gamma_\infty)3eQV_{ZZ}/2I(2I-1)h$ and η_Q are calculated. γ_∞ is the Sternheimer anti-shielding factor which takes into account the EFG induced by the gallium electronic cloud distortion. Due to the Ga^{3+} fluorine octahedral environment, we neglect the anti-shielding anisotropy and assume the scalar Sternheimer constant, $\gamma_\infty = -9.5$ determined for free Ga^{3+} [22].

4.2. Molecular dynamics (MD)

The amorphous GaF_3 structure was simulated using MD calculation [23] as it was previously done to compute EPR parameter distributions [6]. Details about the method were previously described [6, 23]. Two kinds of calculation were achieved: the initial set of atomic positions is either generated at random or obtained from the rhombohedral crystallized GaF_3. The former one was previously applied to account for the x-ray diffraction spectrum of amorphous GaF_3 [23] but was not checked on experimental results sensitive to short range ordering. The latter one was applied to account for EPR spectra of Cr^{3+} and Fe^{3+} doped amorphous GaF_3 and PZG glasses [6]. In this case, it may be kept in mind that it will be impossible to prove the frustrated topology that was suggested in FeF_3 by Mössbauer spectrometry [3, 4].

When the initial set of atomic positions corresponds to crystallized GaF_3, the 'temperature T' is the main parameter of the calculation. It fixes the total energy of the system $E = \frac{3}{2}NkT$ where N is the total number of atoms. The higher the temperature, the faster the ions move away from their initial positions and the larger the generated octahedron distortions. Table 1 gathers the mean values and the standard deviations of the Ga^{3+}–F^- distance and F–Ga–F angle distributions within $(GaF_6)^{3-}$ octahedra at different 'temperatures'. Figure 2 displays such distributions at '300 K'. 80% of the F–Ga–F angles are distributed around 90° (labelled α in table 1, corresponding to orthogonal bonds) and 20% near 180° (labelled β in table 1, corresponding to opposite bonds). These distributions were obtained using initial atomic positions generated from three blocks of 32 unit cells (in a (10 Å)^3 cubic cell) of crystallized GaF_3, corresponding to 576 octahedra (2304 atomic positions). The computation time was about 8 min for each block on a personal computer with an 133 MHz Intel Pentium microprocessor. We recall that the EPR fine structure parameter distribution allowing us to simulate EPR spectra of Cr^{3+} and Fe^{3+} doped amorphous GaF_3 was obtained for '$T = 120$ K'.

For calculations performed from an initial set of random atomic positions of the same size, the distance and angle distributions are given in figure 3. The mean values and the standard

Table 1. Mean values and standard deviations (st. dev.) of the radial and angular distributions obtained by MD. $\langle\alpha\rangle$ and $\langle\beta\rangle$ stand for mean values of the two kinds of F–Ga–F angle in GaF_6 octahedra.

	$\langle d_{Ga-Fe}\rangle$	Radial st. dev. (Å)	$\langle\alpha\rangle$	St. dev. from 90° (°)	$\langle\beta\rangle$	St. dev. from 180° (°)
'10 K'	1.887	0.008	90.00	1.51	178.1	2.27
'75 K'	1.888	0.021	90.00	2.36	176.7	3.76
'120 K'	1.888	0.026	89.99	3.00	175.7	4.84
'200 K'	1.890	0.035	89.99	3.90	174.4	6.36
'300 K'	1.893	0.042	89.98	4.83	173.0	7.89
'500 K'	1.898	0.056	89.96	6.51	170.4	10.76
'random'	1.993	0.110	91.17	17.02	153.5	29.37

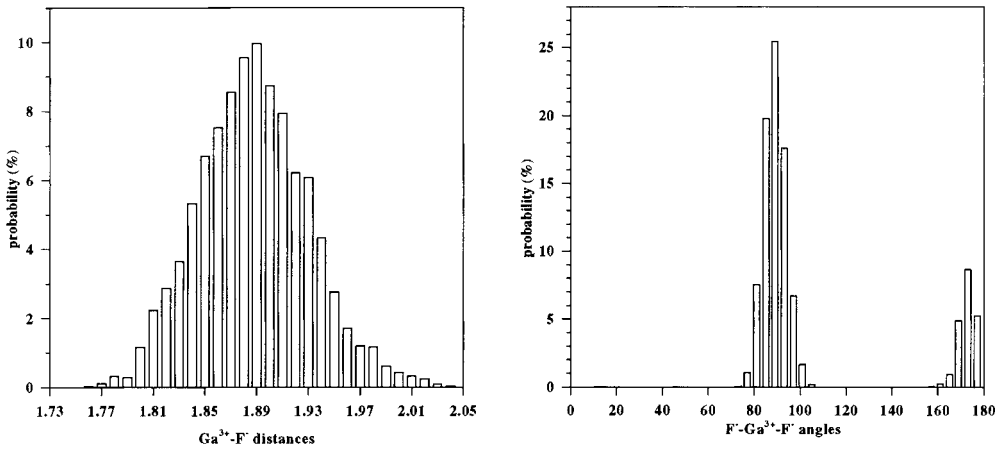

Figure 2. Ga–F distance and F–Ga–F angle distributions in $(GaF_6)^{3-}$ octahedra obtained by MD calculations at '300 K' starting from the rhombohedral GaF_3 phase.

deviations are given in table 1 on the line entitled 'random'. The radial distribution is at least twice broader than in the previous case, and the two angle distributions overlap significantly. These features are consistent with strongly distorted octahedra.

Actually, much larger sets of atomic positions should be used in order to reach convergence at each step of the calculation. Unfortunately, the MD computation time is growing very fast with the number of $(GaF_6)^{3-}$ octahedra taken into account. So, the number of ions chosen in the following calculations is based on a compromise between accuracy and practicability. It will be demonstrated that large MD computation times may be avoided and relevant calculations can be done from the 2304 atomic positions obtained with short time MD calculations. The convergence of the EFG calculations and the correctness of the various approximations will be examined using an unique large set of atomic positions generated from a block of 864 unit cells of crystallized GaF_3, corresponding to 5184 octahedra (20 736 atomic positions) inside a $(60\ Å)^3$ cubic cell. It was previously shown that this size is sufficient to reach convergence in crystals [3]. This was also checked by us on crystallized GaF_3. For this unique data set, the 'temperature' was arbitrarily chosen equal to '300 K'. The computation time reaches nearly 4 days.

4.3. Monopolar approximation

In the monopolar approximation, the EFG can be determined directly from equation (2). We begin to check the convergence of the quadrupolar parameter distribution calculation in this

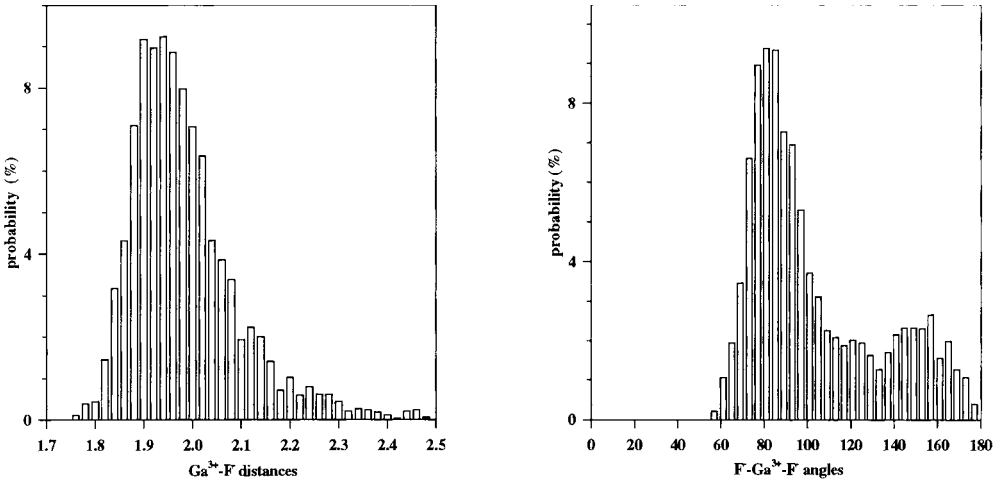

Figure 3. Ga–F distance and F–Ga–F angle distributions in $(GaF_6)^{3-}$ octahedra obtained by MD calculations starting from random initial atomic positions.

approximation by using the large set of atomic positions obtained at '300 K'. Let S_1 be the largest sphere of 30 Å radius included in the box containing all the atoms. In order to check the influence of the radius of the integration sphere S_i which contains the ions labelled λ in equation (2) we perform summations over these λ ions inside nine different integration spheres S_i with radii varying between 2.2 and 18 Å. Taking into account that the largest radius of S_i is equal to 18 Å, EFG monopolar contributions can be calculated only over the 160 Ga^{3+} ions, labelled μ in equation (2), which are inside the S_2 sphere of 12 Å radius in the centre of S_1. It may be noticed that the smallest sphere S_i contains only the 6 F^- nearest neighbours of a central Ga^{3+}. These calculations prove the ν_Q frequency distribution to be practically independent of the size of the integration sphere [24]. From this result, two conclusions were drawn: (a) a calculation using only the 6 F^- nearest neighbour contributions is sufficient to construct the quadrupolar parameter distributions and simulate the experimental spectrum; (b) but, such a calculation is sensitive to short range order only and then insensitive to any topological disorder or medium range order.

This proves that relevant results at the monopolar approximation may be obtained from small atomic position sets. Then, the sets of 2304 atomic positions presented in the previous section may be used to perform EFG calculations. For the sets obtained at '120 K', '300 K' and '500 K', the related quadrupolar parameter distributions and NMR spectra are shown in figures 4(a)–(c). Whatever the 'temperature', the shape of the distributions looks like the Czjzek ones. However all the calculated spectra are too much narrow. The width of the Czjzek distribution used to simulate the experimental NMR spectrum is 4.5 and 2.0 times larger than that of the distributions calculated for '120 K' and '500 K' respectively. In contrast, when EFG calculation is performed from the atomic position set obtained from initial random atomic positions, the calculated spectrum is found to be very similar to the experimental one (figure 4(d)). In this case, the broad radial and angular distributions (table 1, 'random') are not so far from those obtained for the random network of corner sharing octahedra representing the amorphous structure of FeF_3 where both a radial standard deviation of 0.05 Å and an α standard deviation of 13° were found [3]. It should be recalled that the corresponding EFG calculations were carried also in the monopolar approximation. Nevertheless, the 'random' radial and angular distributions are in disagreement with previous results obtained by EXAFS

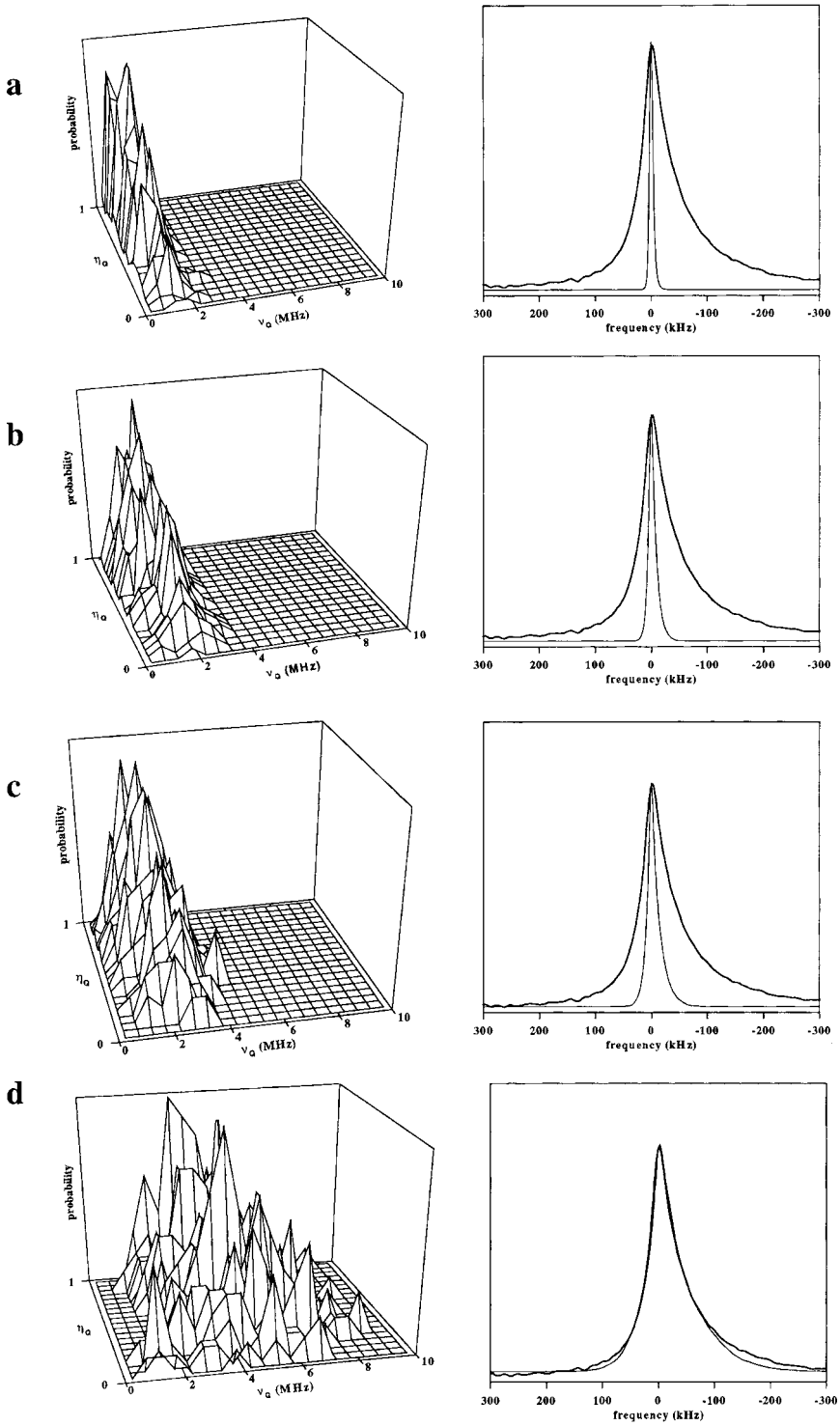

Figure 4. Quadrupolar parameter distributions and related simulated NMR spectra calculated from MD data at '120 K' (a), '300 K' (b), '500 K' (c) and 'random' (d) in the monopolar approximation. The experimental spectrum (thick solid line) is compared to the calculated ones (thin solid line).

[25], Raman [26] and EPR [6] studies which predicted only slightly distorted octahedra. This disagreement with previous results might be explained by the inadequacy of the monopolar approximation. The calculations in the dipolar approximation are developed in the next section.

4.4. Dipolar approximation

The general calculation method may be split into three stages:

- First, the $E_i(\mu)$ electric fields are calculated at the monopolar approximation.
- Next, the total electric fields (i.e. at the dipolar approximation) are evaluated using an iterative method with the $E_i(\mu)$ as initial values for $E_k(\lambda)$ in equation (1). The precision is better than 0.5%.
- Finally, the V_{ij} are calculated according to equation (2).

When we want to carry out these calculations, a difficulty arises from the fact that relations (1) and (2) take into account the electronic polarizabilities denoted $\alpha_e(Ga^{3+})$ and $\alpha_e(F^-)$ and that these parameters are far from settled. Table 2 gathers all the $\alpha_e(F^-)$ values encountered in literature [19, 27–33]: they range from 0.79–1.62 Å^3. Our calculations are based on the following assumptions. First, $\alpha_e(F^-)$ is considered as an adjustable parameter. Next, the value of $\alpha_e(Ga^{3+})$ is deduced from $\alpha_e(Zn^{2+})$ using the Shanker relation [34] which states that as Zn^{2+} and Ga^{3+} have the same electronic configuration, $\alpha_e(Zn^{2+})/\alpha_e(Ga^{3+}) = (r_{Zn^{2+}}/r_{Ga^{3+}})^3$. With $r_{Zn^{2+}} = 0.89$ Å, $r_{Ga^{3+}} = 0.76$ Å [35] and $\alpha_e(Zn^{2+}) = 0.5$ Å [28], one obtains $\alpha_e(Ga^{3+}) \approx 0.3$ Å^3. Finally, a constant ratio between $\alpha_e(Ga^{3+})$ and $\alpha_e(F^-)$ is assumed: $\alpha_e(F^-)/\alpha_e(Ga^{3+}) = 0.8/0.3 = 2.67$ [28].

Table 2. Values of the F^- polarizability from the literature (in Å^3).

[27]	[28]	[29]	[30]	[19]	[31]	[32]	[33]
1927	1965	1973	1976	1982	1984	1985	1992
1.04	0.81	0.87	1.38	0.79–0.90	0.89–1.36	0.92–1.12	1.62

4.4.1. Direct calculation. The first step consists in calculating the electric field in the dipolar approximation. As above, the '300 K' large set of atomic positions is used with the S_1 sphere of 30 Å radius containing all the useful atomic positions. We checked that an integration sphere S_i of 10 Å radius is sufficiently large to reach convergence for the monopolar electric fields. So, these electric fields can be evaluated for all the ions located inside a sphere S_2 of 20 Å radius in the centre of S_1. Afterwards, using once again integration spheres of 10 Å radius, the total dipolar electric fields can be calculated as a function of the F^- polarizability $\alpha_e(F^-)$ only for the ions inside a sphere S_2' of 10 Å radius in the centre of S_1. S_2' contains 84 Ga^{3+} ions. But, the total electric fields are found in average to be proportional to those obtained in the monopolar approximation. The proportionality coefficient increases with the F^- polarizability value. Thanks to this proportionality, the total electric fields can be directly deduced from the monopolar contributions for each ion inside the sphere S_2 of 20 Å in the centre of S_1. It may be outlined that the number of Ga^{3+} ions contained in S_2 is nearly ten times as large as in S_2'.

In the second step, the EFGs in the dipolar approximation have to be evaluated. As was done for the EFG calculation in the monopolar approximation, we verified that a calculation carried out with only the six F^- first neighbours which corresponds to an integration sphere of 2.2 Å radius gives the same quadrupolar frequency distribution as with larger integration spheres [24]. So as in the monopolar approximation, a calculation using only the six F^- nearest neighbour contributions is sufficient to construct the quadrupolar parameter distributions and to

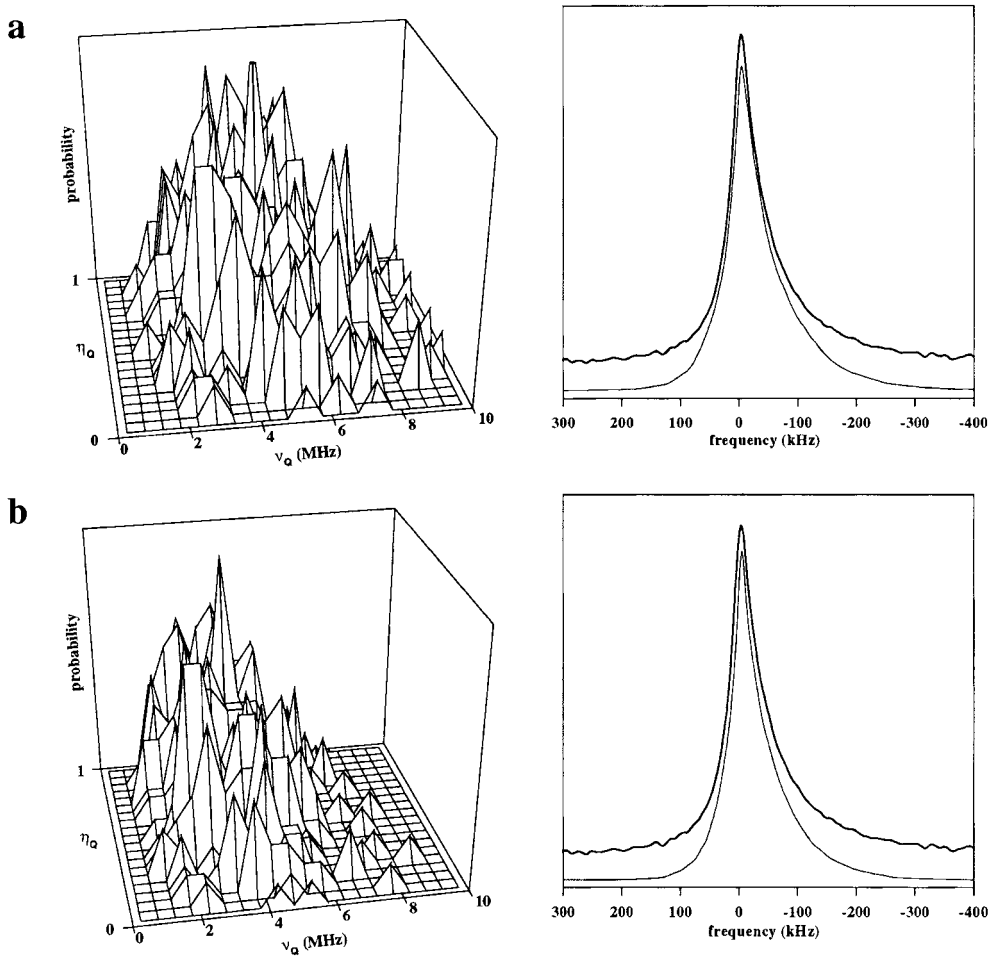

Figure 5. (a) Quadrupolar parameter distribution and related simulated NMR spectra calculated from MD data at '120 K' with $\alpha_e(F^-) = 1.75$ Å^3 in the dipolar approximation. The experimental spectrum (thick solid line) is compared to the calculated one (thin solid line). (b) As (a) at '500 K' with $\alpha_e(F^-) = 0.9$ Å^3.

simulate the experimental spectrum but prevents us from determining any topological disorder or medium range order. Then the EFG can be directly calculated over the 370 Ga^{3+} ions contained in a sphere of 16 Å radius in the centre of S_1 (direct calculation). As this so-called 'direct' calculation can be worked out with a large set of atomic positions only, we proposed a simplified method in order to carry out the calculation from the small sets obtained at various 'temperatures' ('120 K', '300 K' and '500 K').

4.4.2. Simplified method. Thanks to the above direct calculation, we relate the 370 EFG values obtained in the dipolar approximation to those in the monopolar one, versus $\alpha_e(F^-)$. Thus, an average multiplying factor r can be defined for each $\alpha_e(F^-)$ value. Then, using these r factors we are able to infer the quadrupolar frequencies in the dipolar approximation from those calculated in the monopolar one. We find a fairly good agreement between the spectra calculated from both the direct and the simplified methods [24]. This result allowed us to use this simplified method from the small atomic position sets.

Assuming that we may be confident in the γ_∞ and Q values for Ga^{3+} given by literature and taking into account that the F^- polarizability value is far from settled, two approaches are developed with $\alpha_e(F^-)$ as an adjustable parameter:

- In the first one, we assume that the '120 K' MD file is representative of the disorder in amorphous GaF_3 and PZG glasses as found in EPR. To account for the experimental NMR spectrum, $\alpha_e(F^-)$ is found to be equal to 1.75 $Å^3$ corresponding to $r = 4.5$ (figure 5(a)). This value is larger than all those gathered in table 2, but reasonably close to the value 1.62 $Å^3$ given by Shannon in a recent paper [33]. The corresponding quadrupolar parameter distribution is presented in figure 5(a) together with the experimental and calculated NMR spectra.
- In the second one, we assume $\alpha_e(F^-) = 0.9$ $Å^3$ which is in agreement with most of the previous works. Then, $r = 2$ and the '500 K' MD data is found to give the correct quadrupolar parameter distribution which allows the experimental spectrum to be simulated (figure 5(b)). The related angular and radial distributions are broader than in the previous case (table 1) but the octahedra still remain slightly distorted.

It may be surprising to obtain two different distributions (figures 5(a) and 5(b)) which enable us to account accurately for the experimental spectrum. However a similar result has also been noticed when reconstructing this spectrum with Czjzek distributions of the quadrupolar parameters: two of them, with $d = 2$ and $\sigma = 4500$ kHz (figure 1(b)) or $d = 3$ and $\sigma = 3500$ kHz (figure 1(c)), allowed us to reconstruct the ^{71}Ga spectrum. We can note that the distribution calculated from the '120 K' (respectively '500 K') atomic position set is comparable to the $d = 2$ (respectively $d = 3$) Czjzek one. Owing to the featureless NMR spectra, this ambiguity cannot be removed by NMR alone. Nevertheless, the atomic positions obtained by MD calculations at '120 K' starting from the crystallized phase of GaF_3 give rise to a fine agreement with EPR and NMR measurements. This prompted us to apply this latter atomic position set in a recent study related to NMR investigation of mechanically milled nanostructured GaF_3 powders [36].

5. Conclusion

Thanks to the shifted echo and VOCS techniques, the broad ^{69}Ga and ^{71}Ga spectra were recorded in amorphous GaF_3. These spectra were found identical to those obtained in PZG glasses and were simulated with continuous quadrupolar parameter Czjzek distributions and an unique Ga^{3+} chemical shift value. From this chemical shift value it was inferred that in the disordered GaF_3 phase, the Ga^{3+} ions are at the centre of fluorine octahedra as it was previously found in several crystallized compounds [12].

In order to quantify the disorder, EFG calculations were undertaken using a polarizable point charge model. Lattice summations were performed on spherical volumes in direct space. Then, NMR spectra of disordered phases of GaF_3 were reconstructed from atomic position data files calculated by MD. The distributions of the quadrupolar parameters have an overall shape very similar to the analytical Czjzek ones. Whatever the approximations used in the EFG calculation, it was shown that only the six F^- nearest neighbours contribute significantly to the quadrupolar parameter distributions in order to simulate the experimental spectra. So, the ^{71}Ga NMR spectra are sensitive to short range order only, allowing a quantitative description of the radial and angular distortions around Ga^{3+} ions but preventing us from determining any topological disorder or medium range order, as previously proposed.

We showed that the width of the distribution is strongly dependent on the approximation used. With a strict point charge model (monopolar approximation), the MD file generated

from initial random atomic positions enabled us to calculate the experimental amorphous GaF_3 spectra, but the relevant octahedron distortions are too much larger than those inferred from previous experimental studies: EXAFS [25], Raman [26] and EPR [6]. The more elaborated polarizable point charge model in the dipolar approximation allowed us to quantify the short range order and recover only slightly distorted octahedra, despite large uncertainties on the ionic polarizability values. From our simulations, it may be concluded that the radial and angular distributions compatible with the amorphous structure of GaF_3 are those related to our MD calculations from rhombohedral GaF_3 initial atomic positions with '$120\ \mathrm{K} \leqslant T \leqslant 500\ \mathrm{K}$' (table 1). So, the most important result is the following: our results are unable to mirror some frustrated topology as seen in magnetic amorphous FeF_3 by Mössbauer spectrometry [3, 4], but allow us to obtain quantitative informations concerning angular and radial distortions of the GaF_6 octahedra. This may be seen as the necessary first step towards a more complete modelling of the amorphous GaF_3 network.

Since the similarity of the Ga NMR spectra in amorphous GaF_3 and PZG glass, these distributions may also account for the local order in transition metal fluoride glasses. In any case, $(GaF_6)^{3-}$ octahedra are only slightly distorted. Then, our results give evidence for short range order in amorphous GaF_3 and TMFG very similar to crystalline structure built up from MF_6 octahedra. Finally, it should be noted that this rather new approach may be applied to any ionic disordered compound which contains quadrupolar nuclei.

Acknowledgment

The authors acknowledge J M Grenèche for helpful discussions related to EFG calculations.

References

[1] Vermillon K E, Florian P and Grandinetti P J 1998 *J. Chem. Phys.* **108** 7274
[2] Bull L M *et al* 1998 *J. Am. Chem. Soc.* **120** 3510
[3] Grenèche J M, Teillet J and Coey J M D 1987 *J. Physique* **48** 1709
[4] Grenèche J M, Varret F and Teillet J 1988 *J. Physique* **49** 243
[5] Legein C, Buzaré J Y, Emery J and Jacoboni C 1995 *J. Phys.: Condens. Matter* **7** 3853
[6] Legein C, Buzaré J Y, Boulard B and Jacoboni C 1995 *J. Phys.: Condens. Matter* **7** 4829
[7] Table by Weil J A and Rao D S in *Bruker Almanac*
Poole C P and Farach H A (eds) 1994 *Handbook of Electron Spin Resonance* (New York: AIP)
Lide D R (ed) 1995 *CRC Handbook of Chemistry and Physics* 76th edn (Boca Raton, FL: Chemical Rubber Company)
[8] Massiot D, Farnan I, Gautier N, Trumeau D, Trokiner A and Coutures J P 1995 *Solid State NMR* **4** 241
[9] Vosegaard T, Massiot D, Gautier N and Jakobsen H 1997 *Inorg. Chem.* **36** 2446
[10] Vosegaard T, Byriel I P, Binet L, Massiot D and Jakobsen H 1998 *J. Am. Chem. Soc.* **120** 8184
[11] Haegele R, Verscharen W and Babel D 1977 *Z. Anorg. Allg. Chem.* **2** 1947
[12] Bureau B, Silly G, Buzaré J Y, Legein C and Massiot D 1999 *Solid State NMR* **14** 181
[13] Massiot D, Farnan I, Gautier N, Trumeau D, Florian P and Grandinetti P J 1995 *J. Chim. Phys.* **92** 1847
[14] Man P P 1986 *J. Magn. Reson.* **67** 78
[15] Man P P 1993 *Appl. Magn. Reson.* **4** 65
[16] Czjzek G, Fink J, Gotz F, Schmidt H, Coey J M D, Rebouillat J P and Liénard A 1981 *Phys. Rev.* B **23** 2513
[17] Czjzek G 1982 *Phys. Rev.* B **25** 4908
[18] Massiot D, Thiele H and Germanus A 1994 *Bruker Rep.* **140** 43
[19] Teillet J, Calage Y and Varret F 1982 *J. Phys. Chem. Solids* **43** 863
[20] Blank H R *et al* 1994 *Z. Naturf.* **49** 361
[21] Newman D J and Urban W 1975 *Adv. Phys.* **24** 793
[22] Sternheimer R M 1963 *Phys. Rev.* **130** 1423
[23] Boulard B, le Bail A, Jacoboni C and Simmons J H 1988 *Mater. Sci. Forum,* **32–33** 61
[24] Bureau B 1998 *Thesis* Université du Maine

[25] Le Bail A, Jacoboni C and de Pape R 1984 *J. Solid State Chem.* **52** 32
[26] Boulard B, Jacoboni C and Rousseau M 1989 *J. Solid State Chem.* **80** 17
[27] Pauling L 1927 *Proc. R. Soc.* A **114** 181
[28] Phillips C S G and Williams R J P 1965 *Chimie Minérale* vol 1 (Dunod Université) p 28
[29] Jaswal S S and Sharma T P 1973 *J. Phys. Chem. Solids* **34** 509
[30] Cooker H 1976 *J. Phys. C: Solid State Phys.* **80** 2078
[31] Fowler P W and Madden P A 1984 *Phys. Rev.* B **29** 1035
[32] Fowler P W and Pyper N C 1985 *Proc. R. Soc.* A **398** 377
[33] Shannon R D 1993 *J. Appl. Phys.* **73** 348
[34] Shanker J, Kumar N and Verma M P 1973 *Indian J. Pure Appl. Phys.* **11** 644
[35] Kaminski A 1990 *Laser Crystals* (Berlin: Springer)
[36] Bureau B, Guerault H, Silly G, Buzaré J Y and Grenèche J M 1999 *J. Phys.: Condens. Matter* **11** L423